

# Identification of Spatial Distribution of Permeability in Dikes by CPTs

Shin-ichi Nishimura

*Professor, Graduate School of Environmental and Life Science, Okayama University, Okayama, Japan*

Kazunari Imaide

*Graduate Student, ditto*

Toshifumi Shibata

*Associate Professor, ditto*

Takayuki Shuku

*Associate Professor, ditto*

**ABSTRACT:** In this study, the spatial variability of the strength and permeability inside and underneath a river dike are addressed. Cone penetration tests (CPTs) were conducted at the river dike site, which has piping histories. In addition, CPTs were conducted in the laboratory as model tests on soil sampled from the river dike site, and permeability tests were also conducted on the same samples. Based on the laboratory tests, the relationship between the CPT results, which include the tip resistance, the side friction, and the pore pressure, and the permeability is derived. The relationship is applied to the in-situ test results. In conclusion, the spatial variability of the strength and permeability of the test site is evaluated with a geostatistical simulation technique.

When heavy rains come, some river dikes breach. The two major causes of breaching are overflow and seepage failure due to piping. In this work, the procedure for detecting the locations that could be at high risk for piping inside the dikes or in their underlying layers is discussed to mitigate the risk.

Although boring and standard penetration tests are usually conducted to examine the inside of soil structures, the interval of the test points must be sparse due to low efficiency and in order to avoid damage to the structures. Consequently, weak locations may be overlooked. To deal with these shortcomings, the cone penetration test (CPT) is used to obtain detailed information on the inside of the dikes or underneath them. The CPT is advantageous in that it makes short-interval exams possible, due to its high efficiency, and it causes little damage to the structures.

To detect the locations of piping risk, the distribution of permeability in the ground must be identified. The relationship between the CPT results and the coefficients of permeability is derived to evaluate the in-situ permeability by CPTs. For this task, model CPTs and permeability tests were conducted with the same soil samples. A regression equation was derived that represents the relationship of the permeability and the CPT results, namely, the tip resistance, and the side friction.

Some previous articles have addressed the permeability derived from CPTs. For example, Robertson (2010) presented the relationship between CPT results and the permeability. Wang and Tong (2014) also predicted the permeability with CPTs and a similar concept. Paradis *et al.*

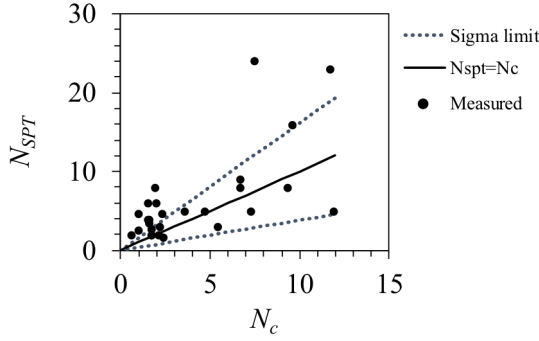


Figure 1. Relationship between  $N_{spt}$  and  $N_c$ .

(2014) used CPT/SMR, and determined the spatial variability of the permeability.

The present study also deals with the spatial variability of the permeability. Firstly, a statistical model is determined from the CPT results to present the spatial distribution of the permeability. Secondly, the permeability inside and underneath a river dike is spatially interpolated by a geostatistical simulation.

## 1. FIELD INVESTIGATION

### 1.1. Cone penetration tests (CPTs)

In the CPTs, tip resistance  $q_t$ , side friction  $f_s$ , and pore water pressure  $P_w$  are measured. Robertson and Fear (1995) proposed a type of soil behavior index,  $I_c$ , based on  $q_t$  and  $f_s$ , which is defined by Equation (1), as follows:

$$I_c = \left\{ (3.47 - \log Q_t)^2 + (1.22 + \log F_R)^2 \right\}^{0.5} \quad (1)$$

$$Q_t = (q_t - \sigma_{v0}) / \sigma'_{v0} \quad (2)$$

$$F_R = f_s / (q_t - \sigma_{v0}) \quad (3)$$

in which  $Q_t$  is the generalized tip resistance,  $\sigma_{v0}$  is the vertical total stress,  $\sigma'_{v0}$  is the vertical effective stress, and  $F_R$  is the generalized side friction ratio (Robertson, 1990).

Suzuki *et al.* (2003) proposed the transformation equation from  $I_c$  and  $q_t$  to the CPT N value,  $N_c$ , as follows:

$$\begin{aligned} N_c &= 0.341 I_c^{1.94} (q_t - 0.2)^{(1.34 - 0.0927 I_c)} & (q_t > 0.2 \text{ MPa}) \\ N_c &= 0 & (q_t \leq 0.2 \text{ MPa}) \end{aligned} \quad (4)$$

The relationship between  $N_c$  and the N value of the standard penetration tests,  $N_{SPT}$ , is based on the data obtained from embankment sites; it is presented in Figure 1. Since the embankment sites have relatively low N values, in the range of 0-10, Equation (5) is defined based on Figure 1. Transformation error  $\epsilon_r$  is also evaluated.

$$N_{SPT} = N_c (1 + 0.62 \epsilon_r) \quad (5)$$

### 1.2. Outline of site

A site investigation was conducted on the Odagawa River dike in Okayama, Japan. A 200-m span along the dike axis was examined, as depicted in Figure 2. As the first step, CPTs were conducted at long intervals of 50 m. As the second step, sounding tests were conducted at short intervals of 5 m. Short-interval tests are definitely required to determine the geostatistical parameters, namely, the lateral correlation lengths.

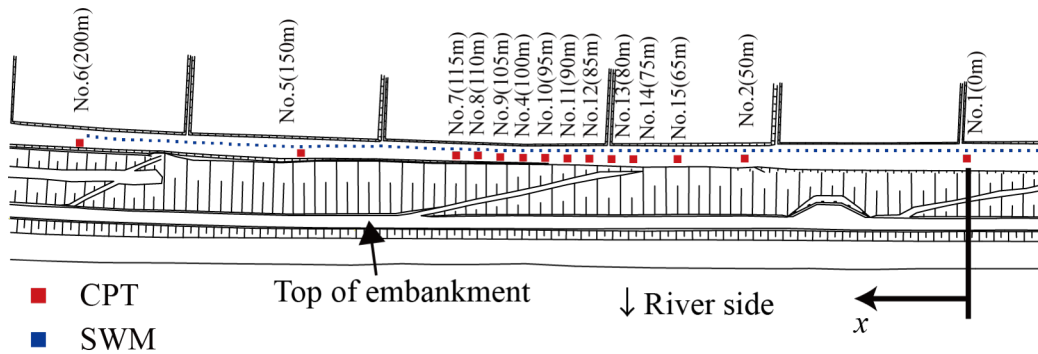


Figure 2. Plan of investigation site.

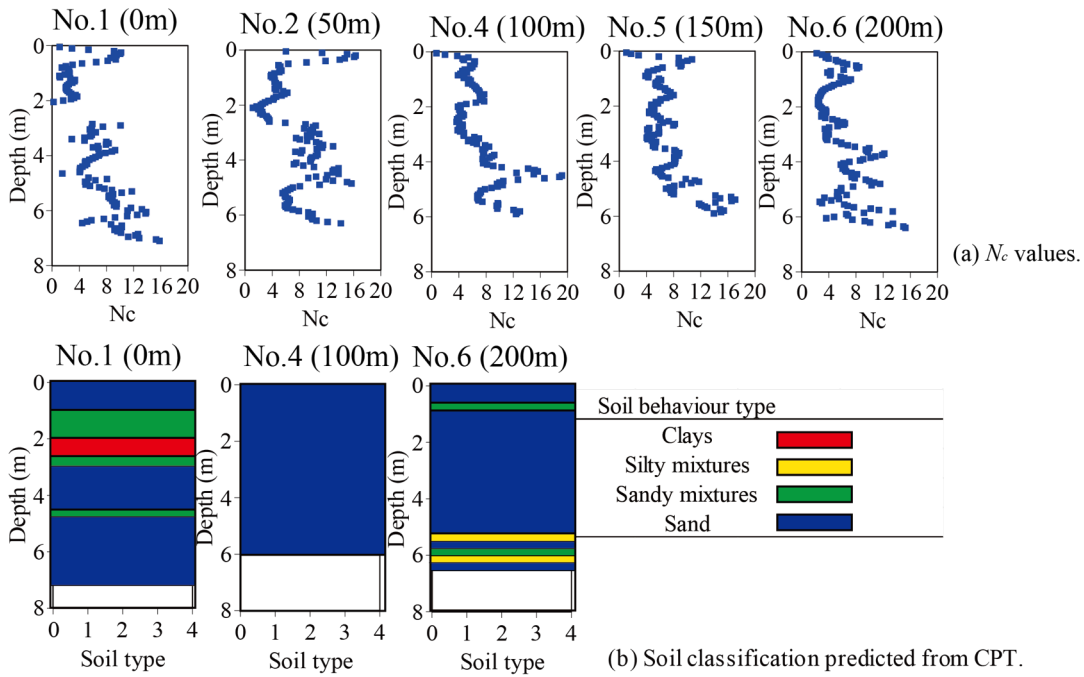


Figure 3. Results of CPTs at Oda River site.

### 1.3. CPT results

In Figure 3(a), the results of the CPTs are given, namely, the CPT N-values,  $N_c$ . According to the figure, there are soft layers at depths around 2 m and 5.5 m. Below the depth of 7 m, the ground is composed of stiff gravel and a sand layer; this does not affect the instability of the dike.

In Figure 3(b), the soil classification is given. The whole area is dominated by the sand layer. Layers of clay or sandy mixtures are found around the depth = 1~2.5 m in the lateral range of  $x=0\sim50$  m, while layers of silty and sandy mixtures are found around the depth 6.0 m at  $x=200$  m.

## 2. MODEL CPTS AND PERMEABILITY TESTS

### 2.1. Test materials and equipment

To create the relationship between the CPT results and the permeability, model CPTs and

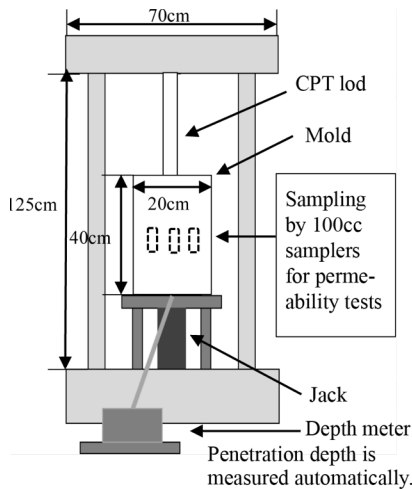


Figure 4. Model test equipment.

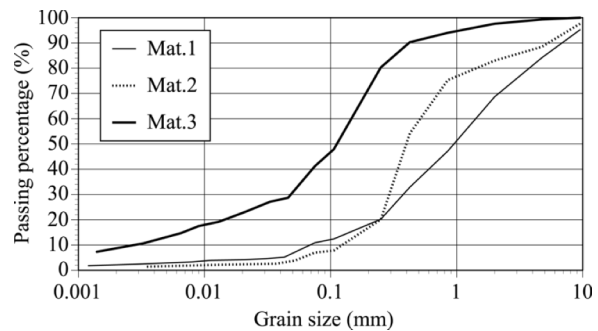


Figure 5. Grain size distribution.

Table 1. Experimental cases and results of CPTs and permeability.

Test Num.	k [m/s]	qt [kPa]	fs [kPa]	pw [kPa]	pt [g/cm <sup>3</sup> ]	e	Sr [%]	w [%]
1- i	1.35E-05	1129.0	11.9	-0.154	1.76	0.649	39.2	9.60
1- ii	1.34E-05	1208.1	18.9	0.111	1.76	0.658	40.0	9.93
1- iii	8.66E-06	1087.7	10.5	-0.245	1.76	0.655	39.3	9.72
1- iv	1.08E-05	1135.8	6.3	0.582	1.75	0.664	40.4	10.13
2- i	5.20E-06	5295.4	35.2	0.263	1.95	0.509	58.5	11.25
2- ii	3.46E-06	7478.6	65.4	4.704	1.96	0.511	61.2	11.80
2- iii	3.90E-06	5171.7	37.6	0.170	1.96	0.573	76.8	12.92
2- iv	6.50E-06	4679.8	35.2	2.088	1.96	0.487	55.5	10.21
3- i	4.33E-06	2559.1	27.1	-0.409	1.91	0.536	52.6	10.66
3- ii	2.60E-06	3005.7	42.7	0.521	1.92	0.525	53.0	10.52
3- iii	3.75E-06	2757.7	22.2	0.021	1.93	0.511	51.4	9.92
3- iv	3.68E-06	2230.1	19.7	0.747	1.84	0.610	51.2	11.80
4- i	4.87E-06	1760.3	14.4	-0.606	1.83	0.595	44.6	10.02
4- ii	4.33E-06	1657.6	8.2	0.903	1.83	0.583	41.8	9.20
4- iii	3.90E-06	1622.6	13.1	0.101	1.80	0.630	44.4	10.56
4- iv	8.23E-06	2105.6	14.2	0.428	1.80	0.625	43.4	10.24
5- i	3.81E-05	6612.1	160.1	-0.485	1.72	0.726	43.0	11.60
5- ii	3.12E-05	8074.0	162.4	0.244	1.72	0.700	41.7	10.85
5- iii	3.64E-05	6731.8	131.8	-0.048	1.79	0.706	33.9	8.88
5- iv	3.12E-05	8178.5	165.4	-2.597	1.77	0.706	44.7	11.72
6- i	3.46E-06	5224.1	121.3	0.170	1.74	0.689	29.1	7.44
6- ii	3.90E-06	5452.5	141.0	0.682	1.76	0.687	28.8	7.34
6- iii	4.33E-06	4010.1	73.8	1.090	1.72	0.635	35.1	8.25
6- iv	2.17E-06	4292.3	102.3	-0.475	1.76	0.645	32.8	7.84

Test numbers 1, 2, 3, and 4: Mat. 1; Test number 5: Mat. 2; Test number 6: Mat. 3.  
The Roman numbers are the repeat numbers.

permeability tests were conducted simultaneously. Figure 4 shows the testing equipment. After the sampled soils are compacted in the mold, the CPTs are conducted. From the compacted soil, the soil specimens are cut out by the 100-cc samplers for the permeability tests. In conclusion, the  $q_t$ ,  $f_s$ , and  $p_w$  values are obtained by the model CPTs, and the permeability is obtained by the permeability tests from the same samples.

The materials are sampled from the Odagawa River site, where piping phenomena have been observed several times due to heavy rains. The grain size distributions are depicted in Figure 5. The three materials, Mats. 1, 2, and 3, have different distributions. Mat. 1 is the finest, while Mat. 3 is the coarsest.

## 2.2. Test results

Mat. 1 is compacted into three degrees of compaction, and the effect of the unit weights is clarified. The initial water content of all the specimens was set to 10%. Table 1 presents the test cases and results.

According to the test results, in cases where the unit weights are almost the same, the permeability increases in the order of Mat. 2, Mat. 3, and Mat. 1. The results correspond to the grain size distributions of the materials. As for the different degrees of compaction, the greater the unit weight of the specimen, the greater the corresponding tip resistance and the smaller the permeability.

From these results in Table 1, permeability  $k$  is derived by Equation (6).

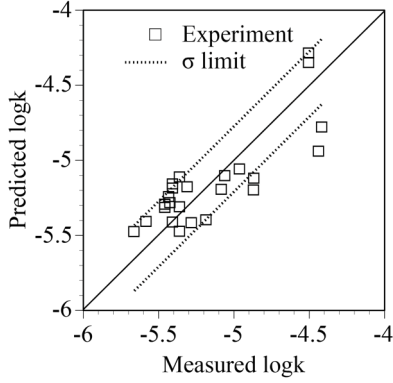


Figure 6. Relationship between measured and predicted permeabilities.

$$\begin{aligned} \log k = & -4.91 - 6.85 \times 10^{-5} q_t \\ & -1.43 \times 10^{-2} f_s - 5.76 \times 10^{-9} q_t^2 \\ & + 1.11 \times 10^{-5} f_s^2 + 2.68 \times 10^{-6} q_t f_s \end{aligned} \quad (6)$$

where the unit of  $k$  is m/s, and the unit of tip resistance  $q_t$  and side friction  $f_s$  is kPa.

Since the degree of saturation in the conducted test cases is low, and the sensitivity of  $p_w$  is supposed to be low, Equation (6) does not include the pore water pressure. The second order regression equation is employed here, since the relatively low order regression is favorable to obtain the mild trend in the extrapolation range of the variables. While, the  $q_t$  and  $f_s$  have the correlation, and therefore, the term  $q_t f_s$  should be included, and second order regression is selected as Equation (6) rather than the linear function.

Figure 6 depicts the relationship of the measured permeability and that predicted by Equation (6). The figure shows that the correspondence between the measured and the predicted permeabilities is relatively good. Transformation error  $\varepsilon_k$  is added to  $\log k$  and the transformed permeability,  $k_T$ , can be evaluated by Equation (7).

$$\log k_T = \log k + \sigma_k \varepsilon_k \quad (7)$$

in which  $\sigma_k=0.246$  is the standard deviation depicted in Figure 6 as the  $\sigma$  limit, and  $\varepsilon_k$  is the  $N(0,1)$  type of normal random variable.

### 2.3. Application to field test results

The  $\log k$ , derived from the in-situ CPT results by Equation (6), is presented in Figure 7. Around the locations of  $x = 50, 85,$  and  $150$  m of  $z = 0 \sim 0.4$  m, the permeability is very high. At  $x = 100$  and  $150$  m of around  $z = 5$  m, there are also high permeability zones.

## 3. STATISTICAL METHODS

### 3.1. Statistical models of spatial variability

A representative variable for the soil properties,  $s$ , which corresponds to  $\log N_c$  or  $\log k$  in this study, is defined by Equation (8) as a function of location  $\mathbf{X}=(x, y, z)$ . Variable  $s$  is assumed to be expressed as the sum of mean value  $m$  and random variable  $U$ , which is a normal random variable in this study.

$$s(\mathbf{X}) = m(\mathbf{X}) + U(\mathbf{X}) \quad (8)$$

The random variable function,  $s(\mathbf{X})$ , is discretized spatially into random vector  $\mathbf{s}^t=(s_1, s_2, \dots, s_M)$ , in which  $s_k$  is a point estimation value at location  $\mathbf{X}=(x_k, y_k, z_k)$ . The soil parameters, which are obtained from the tests, are defined here as  $\mathbf{S}^t=(S_1, S_2, \dots, S_M)$ . Symbol  $M$  signifies the number of test points. Vector  $\mathbf{S}$  is considered to be the realization of random vector  $\mathbf{s}^t=(s_1, s_2, \dots, s_M)$ . If variables  $s_1, s_2, \dots, s_M$  constitute the  $M$ -variate normal distribution, the probability density function of the variable,  $s$  can then be given by the following equation:

$$f_s(\mathbf{s}) = (2\pi)^{-\frac{M}{2}} |\mathbf{C}|^{-\frac{1}{2}} \exp \left\{ -\frac{1}{2} (\mathbf{s} - \mathbf{m})' \mathbf{C}^{-1} (\mathbf{s} - \mathbf{m}) \right\} \quad (9)$$

in which  $\mathbf{m}^t=(m_1, m_2, \dots, m_M)$  is the mean vector of random vector  $\mathbf{s}^t=(s_1, s_2, \dots, s_M)$ ; it is assumed to be the following regression function. In this research, a 2-D statistical model is considered, namely, horizontal coordinate  $x$ , which is parallel to the embankment axis, and vertical coordinate  $z$  are introduced here. The element of the mean vector is described as

$$m_k = a_0 + a_1 x_k + a_2 z_k + a_3 x_k^2 + a_4 z_k^2 + a_5 x_k z_k \quad (10)$$

in which  $(x_k, z_k)$  means the coordinate corresponding to the position of parameter  $s_k$ , and  $a_0, a_1, a_2, a_3, a_4$ , and  $a_5$  are the regression coefficients.

$\mathbf{C}$  is the  $M \times M$  covariance matrix, which is selected from the following four types in this study:

$$\mathbf{C} = [C_{ij}]$$

$$= \begin{cases} \sigma^2 \exp\left(-\frac{|x_i - x_j|}{l_x} - \frac{|z_i - z_j|}{l_z}\right) & \text{(a)} \\ \sigma^2 \exp\left\{-\frac{(x_i - x_j)^2}{l_x^2} - \frac{(z_i - z_j)^2}{l_z^2}\right\} & \text{(b)} \\ \sigma^2 \exp\left\{-\sqrt{\frac{(x_i - x_j)^2}{l_x^2} + \frac{(z_i - z_j)^2}{l_z^2}}\right\} & \text{(c)} \\ N_e \sigma^2 \exp\left(-\frac{|x_i - x_j|}{l_x} - \frac{|z_i - z_j|}{l_z}\right) & \text{(d)} \end{cases} \quad (11)$$

$$i, j = 1, 2, \dots, M$$

$$\begin{cases} N_e = 1 & (i = j) \\ N_e \leq 1 & (i \neq j) \end{cases}$$

in which the symbol  $[C_{ij}]$  signifies an  $i$ - $j$  component of the covariance matrix,  $\sigma$  is the standard deviation, and  $l_x$ , and  $l_z$  are the correlation lengths for the  $x$  and  $z$  directions, respectively. Parameter  $N_e$  is related to the nugget effect. Akaike's Information Criterion, AIC (Akaike, 1974), is defined by Equation (12) considering the logarithmic likelihood.

$$\text{AIC} = -2 \cdot \max \{ \ln f_s(\mathbf{S}) \} + 2L = M \ln 2\pi + \min \{ \ln |\mathbf{C}| + (\mathbf{S} - \mathbf{m})^t \mathbf{C}^{-1} (\mathbf{S} - \mathbf{m}) \} + 2L \quad (12)$$

in which  $L$  is the number of unknown parameters included in Equation (9). By minimizing AIC (MAIC), the regression coefficients of the mean function, the number of regression coefficients, the standard deviation,  $\sigma$ ,

a type of covariance function, the nugget effect parameter, and the correlation lengths are determined. In other words, the determined parameters and the selected covariance function correspond to the minimum AIC.

For  $\log N_c$  and  $\log k$ , the determined mean and covariance functions are determined by the following equations, respectively:

$\log N_c$ :

$$m = 0.379 + 0.111z \quad (13)$$

$$C(\Delta x, \Delta z) = (0.261)^2 \exp \left\{ -\sqrt{\left(\frac{\Delta x}{10.0}\right)^2 + \left(\frac{\Delta z}{0.48}\right)^2} \right\} \quad (14)$$

$\log k$ :

$$m = -5.23 - 0.0557z \quad (15)$$

$$C(\Delta x, \Delta z) = (0.476)^2 \exp \left\{ -\sqrt{\left(\frac{\Delta x}{15.9}\right)^2 + \left(\frac{\Delta z}{0.46}\right)^2} \right\} \quad (16)$$

### 3.2. Geostatistical simulation method

In the present study, the sequential Gaussian simulation method is conducted; analysis code SGSIM (Deutsch and Journel 1992) is employed for the task. A realization  $\xi_c^{(l)}$  by SGSIM is given by Equation (17); it is conditioned at the sample points so that the realized values coincide with the sample values.

$$\xi_c^{(l)}(x, z) = \xi^*(x, z) + \xi^{(l)}(x, z) - \xi^{*(l)}(x, z) \quad (17)$$

in which  $\xi_c^{(l)}(x, z)$  means that the  $l$ th realization,  $\xi^*(x, z)$ , is an estimated value by kriging, and  $\xi^{(l)}(x, z)$  is the  $l$ th realization without conditioning.  $\xi^{*(l)}(x, z)$  is the kriged estimation using the values of  $\xi^{(l)}(x, z)$  at the sampling points. On the right side of Equation (17), the first item is an estimated value of kriging as an average. The remainder of the second and third items shows an estimation error of kriging. The realization,  $\xi_c^{(l)}(x, z)$  is used as  $\log N_c$  and  $\log k$ . To the generated realizations of  $N_c$ , and  $\log k$ , the transformation errors are

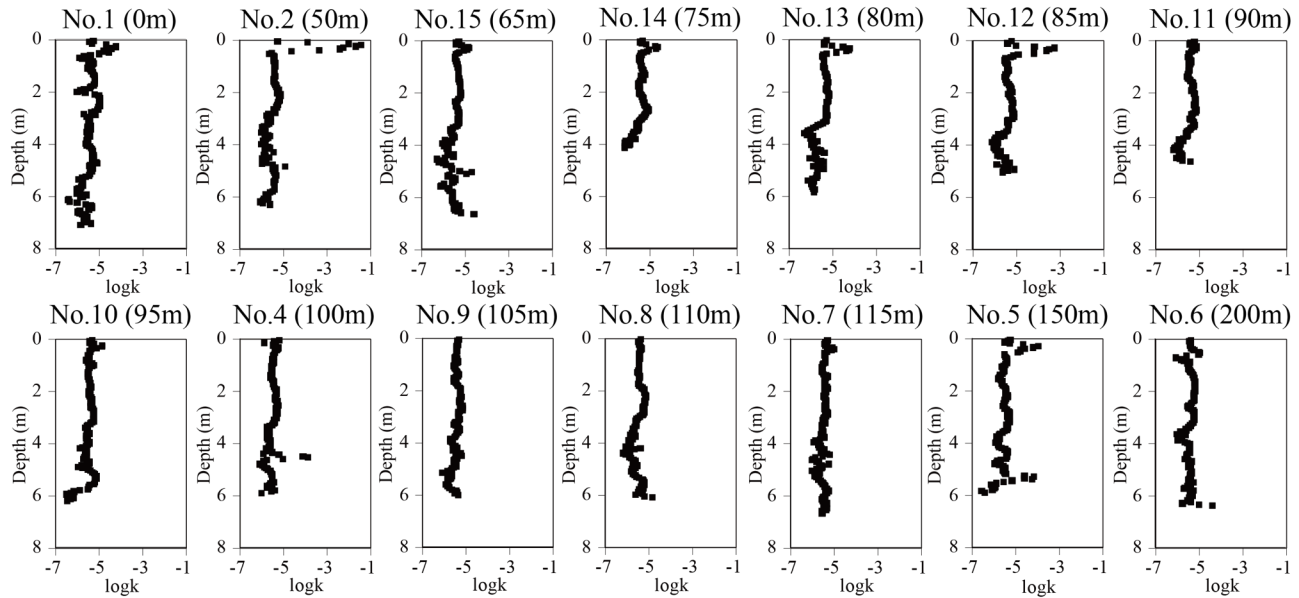


Figure 7. Permeability derived from CPTs at Oda River site.

added, and finally, random numbers for  $N_{SPT}$  and  $\log k_T$  are created. For the random variables, the Monte Carlo simulation is repeated 2000 times.

#### 4. RESULTS OF SIMULATIONS

##### 4.1. Spatial distribution of $N$ values

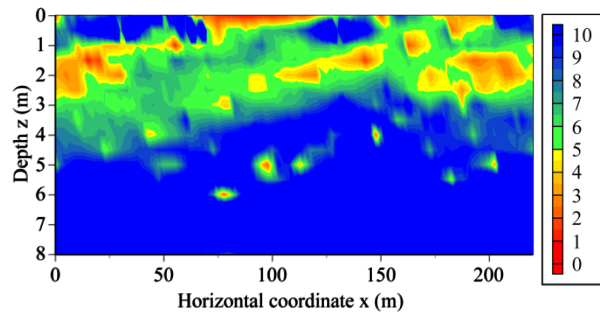
Figure 8 shows the distribution of  $N_{SPT}$  interpolated by the geostatistical simulation. Figures (a), (b), and (c) present the mean, the standard deviation, and the probability of  $N < 5$ , respectively. Weak locations are found around  $x=0\sim 30$  m,  $z=1.5\sim 3.0$  m;  $x=180\sim 210$  m,  $z=1.5\sim 3.0$ ; and  $x=70\sim 120$  m,  $z=0.0\sim 0.3$  m. Except for the span at  $x=30\sim 100$  m, around  $z=1\sim 3$  m, there are weak locations.

##### 4.2. Spatial distribution of permeability

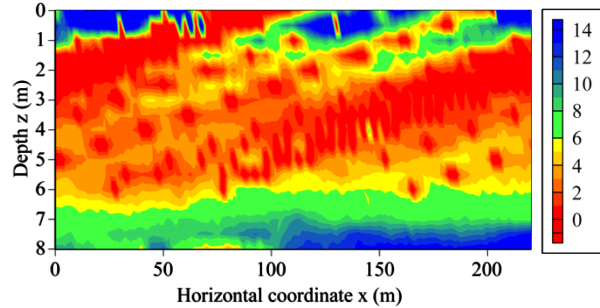
Figures 9(a) and 9(b) present the mean and the standard deviation of transformed permeability  $k_T$ . The trend of the two figures is coincidental. At locations of  $(x$  m,  $z$  m) = (0~40, 0~3), (0~40, 4.5~5.5), (130~180, 0~0.5), (170~190, 1.5~3.5), and (170~190, 4.0~6.5), the possibility of high permeability is great. Considering Figure 8(c), the permeability is high and the strength is low at the locations of  $(x$  m,  $z$  m) = (0~30, 1.5~3) and (180~190, 1.5~3.0). The piping risk is also supposed to be high at these locations.

#### 5. CONCLUSIONS

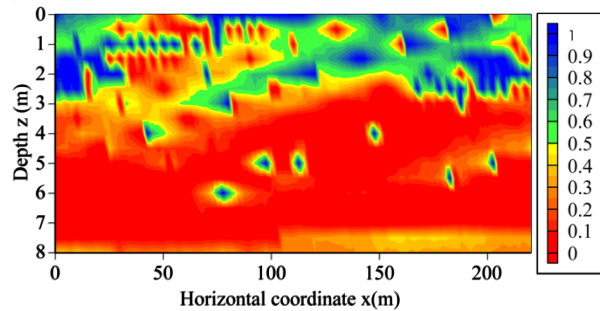
- (1) As a field investigation approach, CPTs were conducted with the long intervals of 50 m, namely, the tests were sparsely conducted. According to the results of the sparse tests, detailed tests with short intervals of 5 m were then scheduled. Based on the detailed tests, it was possible to precisely predict the weak locations and to determine the parameters for the geostatistical modeling.
- (2) To confirm the relationship between the CPT results and the coefficients of permeability, model CPTs and permeability tests were conducted with the same samples. The relationship between the measured permeability and that predicted by the CPTs was derived.
- (3) The statistical models used to present the spatial variability for the  $N$  value and the permeability were reasonably determined from the CPT results.
- (4) As a spatial interpolation method, a sequential Gaussian simulation was employed. With this approach, the weak locations ( $N < 5$ ) and the highly permeable areas were identified. These areas could be at high risk for piping.



(a) Mean



(b) Standard deviation

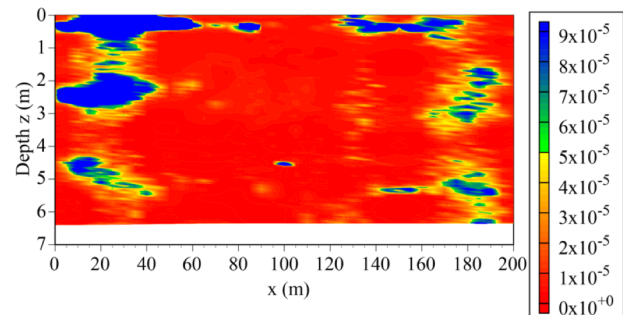


(c) Probability of  $N < 5$

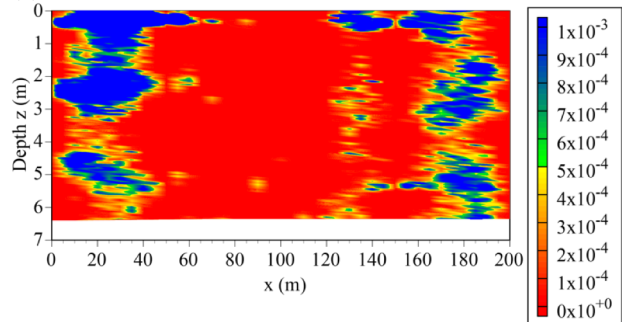
Figure 8. Simulation results for  $N_{SPT}$

## 6. REFERENCES

- Akaike, H. (1974). A new look at the statistical model identification, *IEEE Trans. on Automatic Control*, AC-19(6), 716-723.
- Deutsch, C. V. and Journel, A. G. (1992). *Geostatistical Software Library and User's Guide*, Oxford University Press.
- Paradis, D., Lefebvre, R., Gloaguen, E., and Rivera A. (2014). Predicting hydrofacies and hydraulic conductivity from direct-push data using a data-driven relevance vector machine approach: Motivations, algorithms, and application, *WRR*, 51, 481-505.



(a) Mean



(b) Standard deviation

Figure 9. Simulation results for  $k_T$  (Unit: m/s)

- Robertson P.K. (2010) Estimating in-situ soil permeability from CPT and CPTu, *2nd International Symposium on Cone Penetration Testing*, Huntington Beach, CA, USA.
- Robertson, P. K. (1990). Soil classification using the cone penetration test, *Canadian Geotechnical Journal*, 28(1), 151-158.
- Robertson, P.K. and Fear, C. E. (1995). Liquefaction of sand and its evaluation, *Proc. of 1st. Int. Nat. Symp. on Earthquake Geotechnical Engineering, IS-Tokyo'95*, Vol. 3, 1253-1289.
- Suzuki, Y., Tokimatsu, K. and Sanematsu, T. (2003). Correlations between CPT data and soil characteristics obtained from SPT., *J. Struct. Constr. Eng.*, AIJ, No. 566, 73-80.
- Wang, Q. and Tong, L. (2014) Determination permeability coefficient from piezocone, *Advances in Materials Science and Engineering*, Vol. 2014, Article ID 396428.